Pairing and charge-density-wave correlations in the Holstein model at half-filling

F. Marsiglio
Department of Physics, University of California at San Diego, La Jolla, California 92093
(Received 6 March 1990; revised manuscript received 7 May 1990)

We study the two-dimensional Holstein model at half-filling for small systems using quantum Monte Carlo methods and through diagrammatic perturbation techniques in the Migdal-Eliashberg approximation. It is found that the latter approximation is very accurate as long as the phonon self-energy is taken into account in a self-consistent way. Vertex corrections are not required.

I. INTRODUCTION

In the past few years quantum Monte Carlo techniques have played an important role in understanding simple microscopic models of interacting electron systems. At the same time, since these techniques give essentially exact results for various properties of the system, they provide a standard by which approximate theories can be evaluated. In this paper we wish to investigate the Holstein model, which describes electrons on a lattice which couple to ionic displacements at the lattice sites. This model has previously been investigated with Monte Carlo techniques by Hirsch and Fradkin[1] in one dimension and recently by Scalettar *et al.*[2] in two dimensions. At least in the weak-coupling regime the appropriate theory to describe the pair susceptibility within the Holstein model is the Migdal-Eliashberg (ME) theory.[3] In this theory (see below) explicit vertex corrections are neglected. It is important to realize, however, that in many real applications of Eliashberg theory, vertex corrections are included in an implicit and uncontrolled manner, for example, in the strength of the electron-phonon interaction which is ultimately obtained from experiment, through tunneling inversion.

Similarly, explicit corrections to the phonon propagator are also omitted, since this propagator hardly changes, as a function of temperature, for example, due to the electron-phonon interaction. (Implicit corrections are usually included since the phonon spectrum is often taken from experiment.) While this work is not directly applicable to real materials in that we use a very simple two-dimensional model, it has the merit that electron (and phonon) properties are constructed explicitly from the microscopic parameters, so that direct comparison with Monte Carlo results can be made. In this way the intrinsic importance of vertex corrections can be estimated. It will be seen that at half-filling corrections to the phonon propagator are important, but that once these are taken into account, the Monte Carlo results are well accounted for, even in a situation where charge-density-wave (CDW) correlations are dominant. In the following section we describe the Holstein model in detail. Results for the noninteracting case in two dimensions are also discussed. In Sec. III we describe the Migdal-Eliashberg formalism at two levels of approximation. The first uses the bare phonon propagator as is customarily done, while the second includes a phonon self-energy correction. Scalettar *et al.*[2] used the first approximation, which we will call the "unrenormalized Migdal-Eliashberg" (UME) theory, and compared pairing and charge-density-wave susceptibilities with Monte Carlo results. This was also done (independently) in Ref. 4. We will call the second approximation the "renormalized Migdal-Eliashberg" (RME) theory. In Sec. IV we present results from Monte Carlo (MC) calculations along with comparisons to both levels of approximation, at half-filling, followed by a brief summary in Sec. V. A short report of this work was given in Ref. 4.

II. THE MODEL

A. Hamiltonian

In our calculations, we use the "Holstein" model, with the Hamiltonian

$$H=-\sum_{\substack{ij\\ \sigma}} t_{ij}(c_{i\sigma}^{\dagger}c_{j\sigma}+\text{H.c.})-\mu\sum_{i\sigma} n_{i\sigma} + \sum_{i}\left[\frac{p_i^2}{2M}+\tfrac{1}{2}Kx_i^2\right]-\alpha\sum_{i\sigma} x_i(n_{i\sigma}-\tfrac{1}{2})\,. \tag{1}$$

The Hamiltonian written in this way has particle-hole symmetry for zero chemical potential ($\mu=0$). The parameters entering the model are standard: x_i and p_i are the position and momentum operators for the ion with mass M at site i. The oscillators are taken to be harmonic, with spring constant $K=M\omega_E^2$, each having (unrenormalized) frequency ω_E. The electron kinetic-energy term has hopping-matrix element t_{ij}, usually taken to be nonzero for nearest-neighbor hops only. Finally, α is the electron-phonon coupling parameter, coupling the lattice displacement x_i with the electron density, $n_{i\sigma}\equiv c_{i\sigma}^{\dagger}c_{i\sigma}$, on the same site.

The following assumptions are inherent in the Hamiltonian (1): (1) single band, (2) harmonic approximation for phonons, (3) local approximation for phonons (Einstein model), and (4) on-site electron-phonon coupling only.

As well, we are considering nearest-neighbor hopping

only. This and assumption (1) are easily relaxed. Assumptions (3) and (4) can also be removed, although the simulations become more difficult, and the corresponding Eliashberg equations become more complex. Assumption (2) is most difficult to avoid, although systematic work has already occurred in that direction.

With the simplifying approximations made thus far, Eq. (1) can be Fourier transformed, using the conventional oscillator operators, $a_k=(M\omega_E/2\hbar)(x_k+ip_k)$ ($\hbar\equiv 1$):

$$H=\sum_{k\sigma}\varepsilon_k c^\dagger_{k\sigma}c_{k\sigma}+\omega_E\sum_k(a^\dagger_k a_k+\tfrac{1}{2}) -\frac{\alpha}{\sqrt{2NM\omega_E}}\sum_{\substack{kk'\\ \sigma}}(a_{k-k'}+a^\dagger_{-(k-k')})c^\dagger_{k'\sigma}c_{k\sigma}\ . \tag{2}$$

Here, the momentum sums extend over the first Brillouin zone (FBZ), and

$$\varepsilon_k=-2t(\cos k_x+\cos k_y)-\left[\mu-\frac{\alpha^2}{K}\right]\ .$$

B. The noninteracting case

The noninteracting case has been previously discussed by many authors, but we include it here for completeness. The electron density of states is

$$N(\varepsilon)=\frac{1}{2\pi^2 t}K\left[1-\left[\frac{\varepsilon}{4t}\right]^2\right],\quad |\varepsilon|<4t\ , \tag{3}$$

where K is the complete elliptic integral of the first kind. As a result of two-dimensional (2D) topology on a lattice there is a logarithmic singularity at $\varepsilon=0$. Note that the "textbook" constant density of states comes from a free-electron model with parabolic band and no upper energy cutoff. For our nearest-neighbor-hopping approximation, it is important to realize that in the half-filled case ($\mu=0$) there is the added feature of perfect nesting for $\mathbf{q}=(\pi,\pi)$. As a result, the noninteracting CDW susceptibility at this wave vector is enhanced, and, in the interacting case, Migdal's "theorem" may be violated (see the discussion in Ref. 5).

In this paper we will focus on the singlet pairing (SP) and charge-density-wave susceptibilities. The pairing susceptibility (at $\mathbf{q}=0$) is given by the two-particle Green's function:[6]

$$\chi^{\mathrm{SP}}=\frac{1}{N}\sum_{ij}\int_0^\beta d\tau\langle c_{i\uparrow}(\tau)c_{i\downarrow}(\tau)c^\dagger_{j\downarrow}(0)c^\dagger_{j\uparrow}(0)\rangle \tag{4}$$

which is evaluated using Wick's theorem in terms of single-particle Green's functions. The CDW susceptibility is similarly given by

$$\chi^{\mathrm{CDW}}(\mathbf{q})=\frac{1}{N}\sum_{\substack{ij\\ \sigma\sigma'}}e^{i\mathbf{q}\cdot(\mathbf{R}_i-\mathbf{R}_j)}\times\int_0^\beta d\tau[\langle n_{i\sigma}(\tau)n_{j\sigma'}(0)\rangle-\langle n_{i\sigma}(\tau)\rangle\langle n_{j\sigma'}(0)\rangle]\ . \tag{5}$$

In Fig. 1 we plot $\chi^{\mathrm{CDW}}[\mathbf{q}=(\pi,\pi)]$ and χ^{SP} for the noninteracting case to illustrate the effect of nesting.

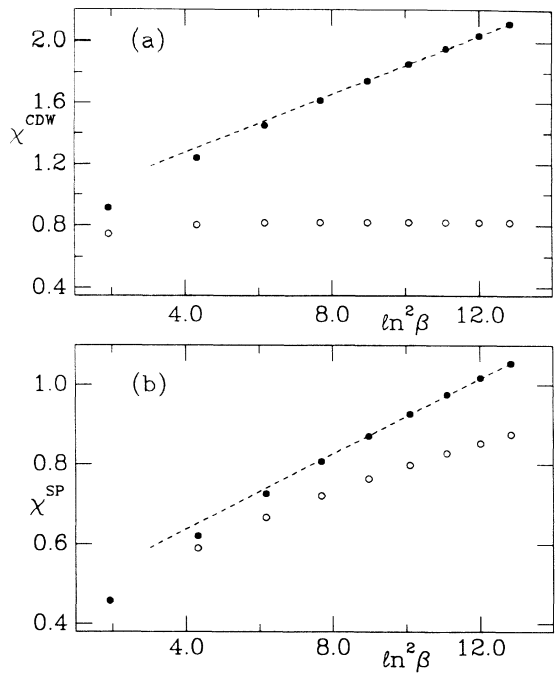

FIG. 1. Plot of (a) $\chi^{\mathrm{CDW}}(\pi,\pi)$ and (b) χ^{SP} vs $\ln^2\beta$, for the half-filled noninteracting case. We have used $N=(4\beta)^2$, where N is the number of sites on the lattice in order to eliminate finite-size effects (Ref. 6). The solid circles are for nearest-neighbor hopping only. The logarithmic singularity gives rise to a $\ln^2\beta$ instability in both the pairing and CDW susceptibilities. The open circles are for a parabolic-like band structure. $\chi^{\mathrm{CDW}}(\pi,\pi)$ has been suppressed completely, while a logarithmic divergence remains for χ^{SP}.

With nearest-neighbor hopping only, both the CDW and SP susceptibilities exhibit $\ln^2\beta[\beta\equiv(k_BT)^{-1}]$ divergences in the half-filled case.[7] Also shown are results using the free-electron-like band structure

$$\varepsilon_k=2t'\sum_{n=1}^{N}\frac{(-1)^n}{n^2}[\cos(nk_x)+\cos(nk_y)]\ ,$$

where t' is determined to give the same bandwidth of $8t$. A cutoff of $N=7$ gives a very good $\sim k^2$ dispersion for most of the Brillouin zone. The figure shows the result for half-filling. The CDW susceptibility is clearly suppressed, while the SP susceptibility is reduced as well; however, in the latter case a logarithmic divergence remains. In the interacting case we can, in general, avoid the nesting condition by remaining well away from the half-filled case.

III. THEORETICAL BACKGROUND

We wish to compute the one-electron Green's function

$$G(\mathbf{k},i\omega_m)=[i\omega_m-\varepsilon_k-\Sigma(\mathbf{k},i\omega_m)]^{-1}\ , \tag{6}$$

where $i\omega_m\equiv i\pi T(2m-1)$ are the fermion Matsubara frequencies and $\Sigma(\mathbf{k},i\omega_m)$ is the electron self-energy due to the electron-phonon interaction. (We use $k_B\equiv\hbar\equiv 1$, and all energies are expressed in units of the hopping, t.)

The Migdal approximation is

$$\Sigma^M(\mathbf{k},i\omega_m) = -\frac{\alpha^2}{N\beta}\sum_{k',m'} D(\mathbf{k}-\mathbf{k}',i\omega_m - i\omega_{m'})G(\mathbf{k}',i\omega_{m'}) , \tag{7}$$

where $D(\mathbf{q},i\nu_n)$ ($i\nu_n \equiv i2\pi Tn$) is the phonon propagator

$$D(\mathbf{q},i\nu_n)=[-M(\omega_E^2+\nu_n^2)-\Pi(\mathbf{q},i\nu_n)]^{-1} . \tag{8}$$

Here $\Pi(\mathbf{q},i\nu_n)$ is the phonon self-energy. As mentioned in the Introduction, in the Eliashberg equations it is customary to omit corrections to the phonon propagator, since usually the phonons are given from experiment, or from a theoretical computation in which the electron-phonon interaction has already been included in the phonon properties. Moreover, it is common practice to use the noninteracting Green's function in place of the fully interacting one in Eq. (7). For a constant density of states and assumed infinite bandwidth ($t \to +\infty$) this is, in fact, exact, so that the approximation is justified for many real materials. For our model we will retain Eq. (7), however, as it is given. Computations have been performed using Eq. (8) both with $\Pi(\mathbf{q},i\nu_n)$ set equal to zero (unrenormalized case) and with $\Pi(\mathbf{q},i\nu_n)$ given by the self-consistent expression (renormalized case):

$$\Pi(\mathbf{q},i\nu_n)=\frac{2\alpha^2}{N\beta}\sum_{k,m} G(\mathbf{k},i\omega_m)G(\mathbf{k}+\mathbf{q},i\omega_m+i\nu_n) . \tag{9}$$

Including Eq. (9) in the calculation will be seen to have important effects on the electron propagator. Finally, a Hartree term is also included and given by

$$\Sigma^H(\mathbf{k},i\omega_m)=\frac{2\alpha^2}{N\beta}D(0,0)\sum_{k',m'} G(k',i\omega_{m'})e^{i\omega_{m'}0^+} = \alpha^2 D(0,0) + \frac{2\alpha^2}{N\beta}D(0,0)\sum_{k',m'}\mathrm{Re}G(k',i\omega_{m'}) . \tag{10}$$

This correction is independent of $\mathbf{k}$ and ω_m and so is reabsorbed into the definition of the chemical potential. In particular, it restores the $\mu=0$ condition for the half-filled case, even in the fully interacting case. The graphs used are summarized in Fig. 2.

Defining

$$\Sigma(\mathbf{k},i\omega_n)\equiv i\omega_n[1-Z(\mathbf{k},i\omega_n)]+\chi(\mathbf{k},i\omega_n) \tag{11a}$$

and

$$\frac{\Pi(\mathbf{q},i\nu_n)}{M\omega_E^2}\equiv\Pi_1(\mathbf{q},i\nu_n)-1-\frac{\nu_n^2}{\omega_E^2}+i\Pi_2(\mathbf{q},i\nu_n) , \tag{11b}$$

we obtain four coupled equations for Z, χ, Π_1, and Π_2. For a given occupation n, these are solved to consistency along with the condition

$$n=\frac{2}{N\beta}\sum_{k,m'} G(k',i\omega_{m'})e^{i\omega_{m'}0^+} , \tag{12}$$

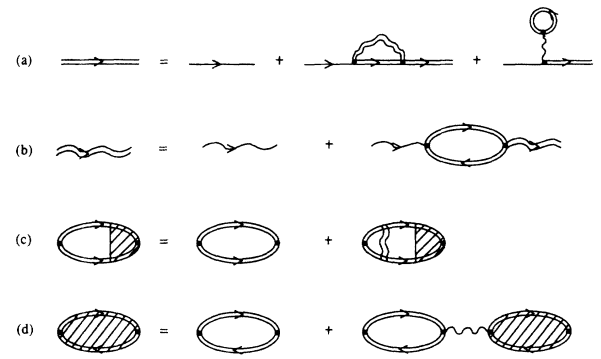

FIG. 2. The Migdal-Eliashberg equations in diagrammatic form. The single and double solid (wavy) lines represent the noninteracting and interacting electron (phonon) Green's function. (a) and (b) determine the self-energies self-consistently, while (c) and (d) represent the ladder and bubble sums for the pairing and CDW susceptibilities, respectively. In the usual unrenormalized ME approximation, the noninteracting phonon Green's function is used everywhere.

which determines the self-consistent chemical potential. These equations are given in the Appendix. For the simplified case $\Pi(\mathbf{q},i\nu_n)\equiv 0$, we obtain the equations

$$\omega_m Z_m = \omega_m + \frac{1}{N\beta}\sum_{k',m'}\lambda_0(i\omega_m - i\omega_{m'}) \times \frac{\omega_{m'}Z_{m'}}{\omega_{m'}^2 Z_{m'}^2+(\varepsilon_{k'}+\chi_{m'})^2} , \tag{13a}$$

$$\chi_m = -\frac{1}{N\beta}\sum_{k',m'}\lambda_0(i\omega_m - i\omega_{m'})\frac{\varepsilon_{k'}+\chi_{m'}}{\omega_{m'}^2 Z_{m'}^2+(\varepsilon_{k'}+\chi_{m'})^2} , \tag{13b}$$

and

$$n=1-\frac{2}{N\beta}\sum_{k',m'}\frac{\varepsilon_{k'}+\chi_{m'}}{\omega_{m'}^2 Z_{m'}^2+(\varepsilon_{k'}+\chi_{m'})^2} . \tag{13c}$$

Here, since $\Pi(\mathbf{q},i\nu_n)=0$, $\chi_m \equiv \chi(i\omega_m)$, and $Z_m \equiv Z(i\omega_m)$ are independent of wave vector, so that the iteration procedure is sped up significantly. The function $\lambda_0(z)$ is defined

$$\lambda_0(z)\equiv\frac{(\alpha^2/M)}{\omega_E^2-z^2} . \tag{14}$$

Equations (13) are the ones solved by Scalettar *et al.*[2] (the m dependence of χ_m turns out to be not too important near half-filling, and they have absorbed χ_m into the definition of the chemical potential; at half-filling, $\chi_m \equiv 0$). We have included the subscript 0 to differentiate this function from the more commonly used (dimensionless) $\lambda(z)$:

$$\lambda(z)\equiv\frac{\lambda\omega_E^2}{\omega_E^2-z^2} . \tag{15}$$

The two are usually simply related by $\lambda(z)=N(0)\lambda_0(z)$,

where $N(0)$ is the normal-state noninteracting (i.e., with phonons) density of electron states at the Fermi level (assumed to be constant over the energy range of interest). Here, however, this simple relation clearly does not hold (at half-filling, λ is not infinite, for example), and we will resort to the fundamental definition

$$\lambda_{\mathbf{k}} \equiv -\left.\frac{\partial \mathrm{Re}\Sigma(\mathbf{k},\omega)}{\partial\omega}\right|_{\omega=E_F} , \tag{16}$$

where $\Sigma(\mathbf{k},\omega+iO^+)$ is the analytic continuation of $\Sigma(\mathbf{k},i\omega_n)$.

Once the self-energies are evaluated one can compute the various susceptibilities to probe the tendencies of the system at a given temperature. In particular, the pairing susceptibility, χ^{SP}, given by Eq. (4), will diverge at the superconducting transition temperature. As noted by Scalettar *et al.*,[2] in 2D this is expected to be a Kosterlitz-Thouless-like transition, which is not described by Eliashberg theory.

Within the ME theory, Eq. (4) is given by summing the infinite series of ladder diagrams. The result is

$$\chi^{\mathrm{SP}} = \frac{1}{N\beta}\sum_{k,m} F_0(\mathbf{k},i\omega_m)\Lambda(\mathbf{k},i\omega_m) , \tag{17}$$

where

$$F_0(\mathbf{k},i\omega_m) = G(\mathbf{k},i\omega_m)G(-\mathbf{k},-i\omega_m) \tag{18}$$

and $\Lambda(\mathbf{k},i\omega_m)$ is the solution of the vertex equation:

$$\Lambda(\mathbf{k},i\omega_m) = 1 - \frac{\alpha^2}{N\beta}\sum_{k',m'} F_0(\mathbf{k}',i\omega_{m'}) \times D(\mathbf{k}-\mathbf{k}',i\omega_m - i\omega_{m'}) \times \Lambda(\mathbf{k}',i\omega_{m'}) . \tag{19}$$

As $T\to T_c$ from above, $\Lambda(\mathbf{k},i\omega_m)\gg 1$, $\chi^{\mathrm{SP}}\to\infty$, and Eq. (19) (with the 1 dropped) becomes the eigenvalue equation that determines T_c, written on the imaginary axis.[8] Again, for $\Pi(\mathbf{q},i\nu_n)\equiv 0$, $\Lambda(\mathbf{k},i\omega_m)\to\Lambda_m$, and Eq. (19) needs to be iterated in imaginary frequency space only. In the nonretarded (NR) limit,

$$D(\mathbf{q},i\nu_n)\to(-M\omega_E^2)^{-1} ,$$

so Eq. (19) decouples, and one obtains the BCS pairing susceptibility

$$\chi^{\mathrm{SP}}_{\mathrm{NR}} = \frac{\chi_0^{\mathrm{SP}}}{1-\lambda_0\chi_0^{\mathrm{SP}}} , \tag{20}$$

where χ_0^{SP} is given by Eq. (17) with $\Lambda(\mathbf{k},i\omega_m)\equiv 1$, and $F_0(\mathbf{k},i\omega_m)$ given in terms of noninteracting Green's functions, and with $\lambda_0\equiv(\alpha^2/M\omega_E^2)$.

The CDW susceptibility is determined in similar fashion, except that only the zero-frequency phonon propagator at wave vector $\mathbf{q}$ enters, so that [for $\Pi(\mathbf{q},i\nu_n)\equiv 0$] one obtains

$$\chi^{\mathrm{CDW}}(\mathbf{q}) = \frac{\chi_0^{\mathrm{CDW}}(\mathbf{q})}{1-\lambda_0\chi_0^{\mathrm{CDW}}(\mathbf{q})} , \tag{21}$$

where $\chi_0^{\mathrm{CDW}}(\mathbf{q})$ is given by the expression in Eq. (9):

$$\chi_0^{\mathrm{CDW}}(\mathbf{q}) = -\frac{\Pi(\mathbf{q},0)}{\alpha^2} . \tag{22}$$

At half-filling, for $\mathbf{q}=(\pi,\pi)$, then $\chi_0^{\mathrm{CDW}}=2\chi_0^{\mathrm{SP}}$, so that Eq. (21) will always diverge sooner than Eq. (20). Moreover, as discussed in Ref. 6, retardation will diminish the enhancement of the denominator in Eq. (20). Furthermore, the self-energy effects from retardation "weigh down" the single particle-hole bubble so that χ_0^{SP} is depressed and χ^{SP} is further reduced. These latter reductions cannot be avoided; however, the competition with Eq. (21) can be readily avoided by going to fillings away from half-filling, or altering the band structure, as already noted.

Equation (22) also indicates that, in using the full equations for Z, χ, Π_1, and Π_2, we are "backfeeding" the CDW tendency into the self-energy equations. Thus, as will be seen in the results, we obtain an immediate signal that the system is unstable to a CDW.

The Monte Carlo algorithm used in this work is that of Blankenbecler *et al.*,[9] with modifications due to Hirsch[10] to give greater stability at lower temperatures. We have concentrated on 4×4 lattices. These small sizes are sufficient for an evaluation of the ME theory (agreement should improve for larger lattices). The ME equations can then be readily solved for much larger lattices.

IV. DISCUSSION OF RESULTS

The Holstein Hamiltonian with nearest-neighbor hopping will not yield superconductivity in the half-filled case in two dimensions. Nonetheless, as discussed by Allen and Mitrovic,[5] this is precisely the situation in which Migdal's theorem is expected to break down, so that ME theory should fail. For this reason, we will concentrate on the half-filled case.

In Fig. 3 we plot the pairing susceptibility χ^{SP} [Eq. (4)]

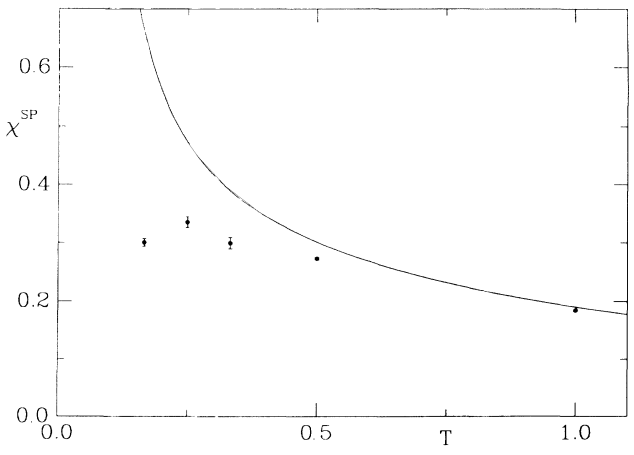

FIG. 3. Plot of the pairing susceptibility χ^{SP} vs temperature, as computed from Monte Carlo (circles) and from unrenormalized ME theory at half-filling. Here, $\lambda_0=2$ and $\omega_E=0.5$. There is significant disagreement, especially at low temperatures. The error bars accompanying the MC results indicate the statistical error.

as obtained from Monte Carlo calculations and from the unrenormalized ME theory (using the bare phonon propagator), for a bare coupling strength $\lambda_0 \equiv \alpha^2/K = 2$, phonon frequency $\omega_E = 0.5$, and filling $n = 1$. All energy units are expressed in terms of the hopping integral t. There is a clear "failure" of the UME theory even for this "weak-coupling" case. The cause of the failure is clear from Fig. 4, where we have plotted the charge-density-wave susceptibility at wave vector $\mathbf{q} = (\pi, \pi)$ (the nesting wave vector), $\chi^{\mathrm{CDW}}(\pi, \pi)$ versus temperature, again for both the Monte Carlo and the UME calculations. Note that the scale differs from that of Fig. 3 by 2 orders of magnitude. The system is clearly approaching a charge-density-wave instability and finite-size effects become prohibitive. When a susceptibility approaches the magnitude indicated in Fig. 4, a larger lattice size is usually required to handle the long-range correlation correctly. The UME approximation has also indicated a CDW instability. While the "bubble" approximation [Eq. (21)] drastically overestimates the CDW susceptibility, it nonetheless serves as a signal that the UME equations will not be reliable below $T \approx 0.7t$. Figure 3 shows that this is indeed the case.

This result makes it clear that the unrenormalized ME theory of the normal-state electron Green's function does not incorporate either the tendency for singlet pairing or the tendency for charge-density-wave formation. When susceptibilities are calculated, however, we find that the CDW instability dominates. The calculation is then meaningless at temperatures below that which yield a sizable CDW susceptibility so that the disagreement in Fig. 3 is expected.

An improvement of the theory consists of improving the agreement in CDW susceptibilities (Fig. 4). We then expect the SP susceptibility to agree more closely with the Monte Carlo result. Towards this end, we have carried out calculations in which a renormalized phonon propagator [Eq. (8)] is self-consistently calculated along with the electron propagator. We use for the phonon self-energy the bubble diagram [Fig. 2 and Eq. (9)], which is given in terms of the self-consistent electron Green's functions. (See the Appendix for calculational details.) The results are given in Fig. 5, for a slightly different set of parameters: $\alpha^2/K = 1.5$ and $\omega_E = 0.5$. Figure 5(a) illustrates the singlet pairing susceptibility, χ^{SP}, calculated by various means. The dotted line represents the noninteracting electron susceptibility and is included for reference. The solid line is the result from the unrenormalized ME theory. Note that the pairing susceptibility is suppressed in the temperature regime indicated, as pointed out previously.[2,4] Calculation to lower temperatures reveals a crossover, with the unrenormalized ME result eventually diverging at a finite temperature. The points indicate the Monte Carlo results. At temperatures below $T/t \approx 0.5$, there is a definite overestimate of the UME theory compared with the MC results. Finally, the dashed line gives the renormalized ME result in very good agreement with the MC results. In Fig. 5(b) we show the same results for $\chi^{\mathrm{CDW}}(\pi, \pi)$. Agreement with the Monte Carlo results is somewhat improved by using the renormalized ME results.

We have chosen these particular parameters because they give a clear indication of what is happening in the

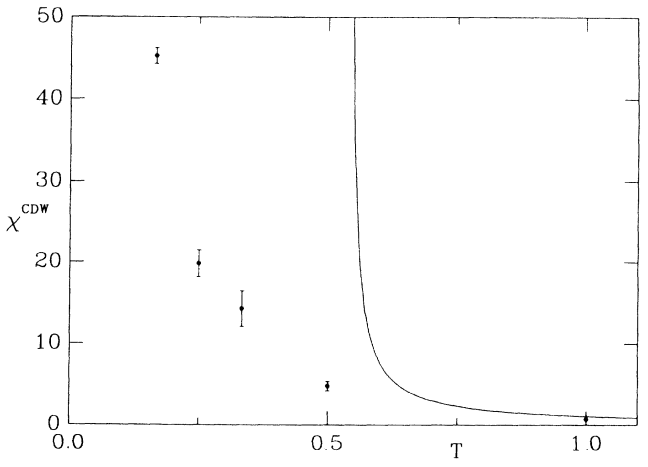

FIG. 4. Plot of charge-density-wave susceptibility $\chi^{\mathrm{CDW}}(\pi, \pi)$ vs temperature. The parameters and legend are the same as Fig. 3. Note the difference in scale compared to Fig. 3. The unrenormalized ME theory drastically overestimates $\chi^{\mathrm{CDW}}(\pi, \pi)$.

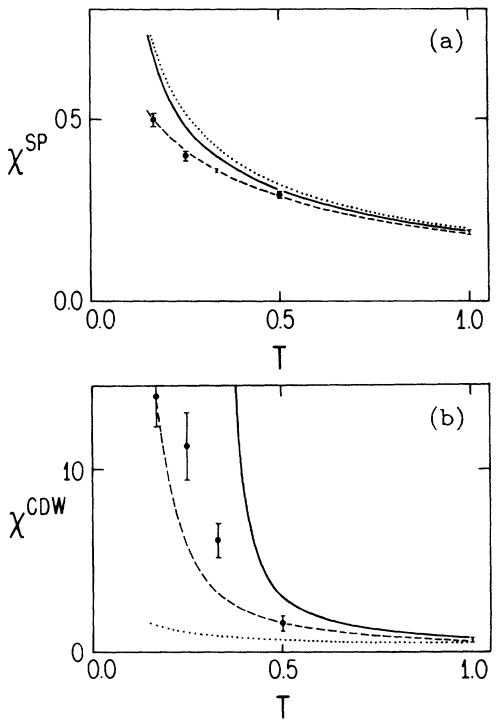

FIG. 5. Plot of (a) χ^{SP} and (b) $\chi^{\mathrm{CDW}}(\pi, \pi)$, calculated by various means for $\lambda_0 = 1.5$, $\omega_E = 0.5$, at half-filling on a 4×4 lattice. The dotted lines indicate the noninteracting result for reference. The circles are the Monte Carlo results, the solid lines are the unrenormalized ME results, and the dashed lines are the renormalized ME results (phonon self-energy self-consistently included). Agreement is markedly improved when the phonon self-energy correction is included, especially in (a).

relevant temperature range. As Scalettar *et al.*[2] have discussed, smaller values of λ_0 will, in general, shift the results of Fig. 5 to lower temperatures, where, however, finite-size effects dominate. Larger values of λ_0 cause the CDW instability to appear at higher temperatures, where deviations from the noninteracting χ^{SP} are not significant. Similarly a lower phonon frequency gives rise to stronger CDW correlations.[6]

The renormalized ME theory differs from conventional Eliashberg theory in that in the former the phonon spectrum changes significantly as a function of temperature. This is best seen in Fig. 6, where we plot $\Pi_1(\mathbf{q},0)$ for $\mathbf{q}=(\pi,\pi)$ versus temperature for the parameters of Fig. 5. Recall that the phonon propagator at zero frequency is $-[1/M\omega_E^2\Pi_1(q,0)]$ rather than $-(1/M\omega_E^2)$, the latter case applying to the unrenormalized theory. This means that the effective λ is given by $\lambda^{\text{eff}}(\mathbf{q})\approx\lambda/\Pi_1(\mathbf{q},0)$. We should stress that $\Pi_1(\mathbf{q},0)$ has been calculated self-consistently, and not just at the end of the unrenormalized calculation. The question then arises: what value of the dimensionless electron-phonon mass enhancement parameter, λ, corresponds to a specific choice of λ_0? We can calculate λ via Eq. (16) exactly in the unrenormalized theory, by solving the analytic continuation equations, derived recently in Ref. 11. In our case, the equation is

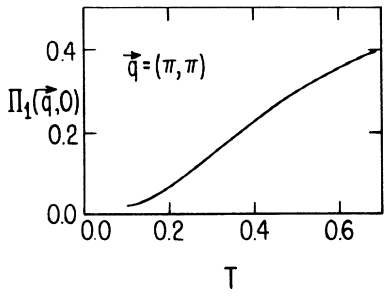

FIG. 6. Plot of the real part of the phonon self-energy $\Pi_1(\mathbf{Q},i\nu_n=0)$ [see Eq. (11b) for definition] for $\mathbf{Q}\equiv(\pi,\pi)$ vs temperature. $\Pi_1(\mathbf{q},0)$ approaches zero as T decreases indicating the formation of a CDW. The effective λ_0 becomes $\lambda_0^{\text{eff}}\approx\lambda_0/\Pi(\mathbf{Q},0)$, and diverges as T decreases.

$$\Sigma(\mathbf{k},\omega+i\delta)=\frac{1}{N\beta}\sum_{k',m'}\lambda_0(\omega-i\omega_{m'})G(\mathbf{k}',i\omega_{m'})+\frac{\lambda_0\omega_E}{2}\left[[N(\omega_E)+1-f(\omega-\omega_E)]\frac{1}{N}\sum_{k'}G(\mathbf{k}',\omega-\omega_E)\right.$$
$$\left.+[N(\omega_E)+f(\omega+\omega_E)]\frac{1}{N}\sum_{k'}G(\mathbf{k}',\omega+\omega_E)\right], \tag{23}$$

where $N(\nu)$ and $f(\nu)$ are the Bose and Fermi functions, respectively. Clearly, $\Sigma(k,\omega)$ is independent of $\mathbf{k}$. Equation (23) is solved by iteration, with the first term given from the imaginary axis calculation. Equation (16) can then be straightforwardly used to determine the dimensionless mass enhancement constant λ. For frequencies of order t, the hopping-matrix element, we always found at low temperatures that $\lambda\approx\lambda_0/D$, where D is the bandwidth. Since $1/D$ is the average value of the density of states, this is not too surprising. An intersting effect, first discussed by Alexandrov *et al.*[12] in the context of the unrenormalized theory, is shown in Fig. 7, where we plot the quasiparticle density of states $N(\omega)$ versus ω for $\lambda_0=1.5$, $\omega_E=0.5$, and $\beta=12$, for a large system (80×80 sites). Smearing has occurred both due to finite temperature and due to the electron-phonon interaction. The noninteracting result is also plotted, using an artificial broadening to avoid the singularities due to the discretization. In the interacting case there is a collapse of the quasiparticle density of states, occurring at the phonon energy, $\omega_E=0.5$. Alexandrov *et al.*[12] claim that this points towards the need for inclusion of vertex corrections, whereas we have argued that only the phonon self-energy correction needs to be included. The claim of Ref. 12 for definite values of the dimensionless electron-phonon coupling constant λ is also in doubt since it is clear from Fig. 6 that the *effective* λ is increasing as a function of temperature, eventually diverging as the CDW instability is approached. In order to shed light on this issue we have examined the electron self-energy both on the imaginary and real axis.

In the first case, recently, Moreo *et al.*[13] have noted

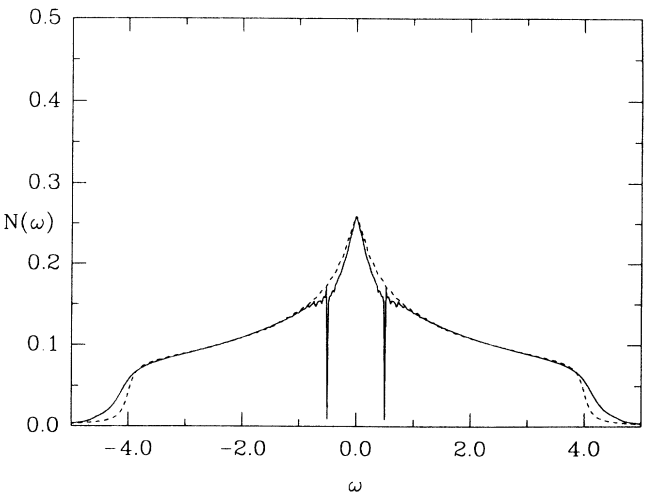

FIG. 7. Plot of the quasiparticle density of states, $N(\omega)$ vs ω for a large system, with $\lambda_0=1.5$, $\omega_E=0.5$, and $\beta=12$, calculated within the unrenormalized ME approximation. The dashed line represents the noninteracting case with artificial broadening. Note the collapse in the density of states at $\pm\omega_E=0.5$.

that the electron self-energy evaluated on the imaginary axis gives important information about the existence of a gap in the one-electron spectrum. Specifically, they have argued that in a Fermi liquid the imaginary part of the self-energy will have a negative slope for small values of ω_n, whereas it will diverge if a gap is forming. In Fig. 8, we show results for a 4×4 system at low temperatures ($\lambda_0=1.5$, $\omega_E=0.5$), for both the unrenormalized and renormalized ME calculations. We have been unable to iterate the renormalized ME equations to lower temperatures due to the CDW instability. Figure 8 shows that while the renormalized ME solutions know of the formation of a CDW gap, the unrenormalized ME solutions do not.

An exact analytic continuation of the electron self-energy in the renormalized ME theory appears to be impossible so we have relied on Padé approximants.[14] In Fig. 9 we plot the spectral function

$$A(\mathbf{k},\omega)\equiv-\frac{1}{\pi}\mathrm{Im}G(\mathbf{k},\omega+i\delta)$$

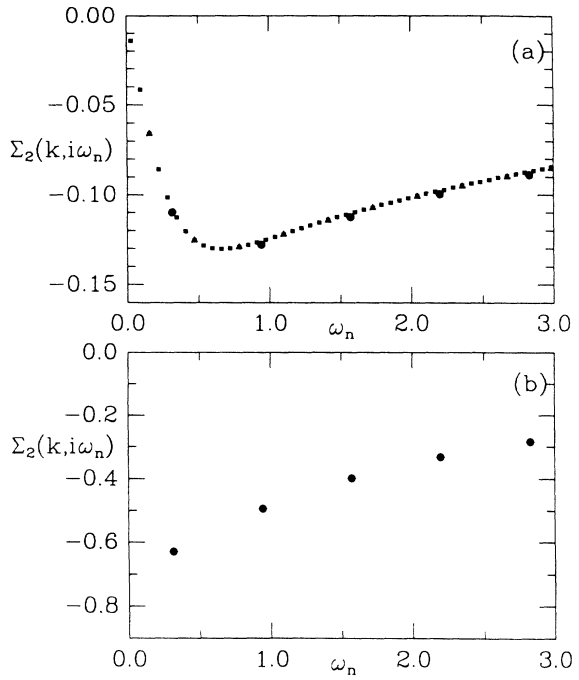

FIG. 8. Plot of the imaginary part of the self-energy on the imaginary axis, $\Sigma_2(\mathbf{k},i\omega_n)\equiv\mathrm{Im}\Sigma(\mathbf{k},i\omega_n)=\omega_n[1-Z(k,i\omega_n)]$ vs ω_n. In (a) we plot the result due to the unrenormalized ME approximation (for $\lambda_0=1.5$, $\omega_E=0.5$, and $N=4\times4$). We show the result for temperatures $\beta=10$, 20, 100. The results are essentially the same except that for $\beta=100$ many more points are filled in, thus indicating that $\beta=10$ is a sufficiently low temperature. Note that this result suggests normal Fermi-liquid behavior, even though CDW correlations are dominant. (The CDW susceptibility has already diverged, for example, within this approximation at $\beta\approx0.5$.) In (b) we plot the result for $\beta=10$ within the renormalized ME approximation at a wave vector on the Fermi surface, $\mathbf{k}=(\pi/2,\pi/2)$. We find the expected behavior (Ref. 13) $\mathrm{Im}\Sigma(\mathbf{k},i\omega_n)\sim-(\Delta^2/\omega_n)$ indicating that a CDW gap is forming.

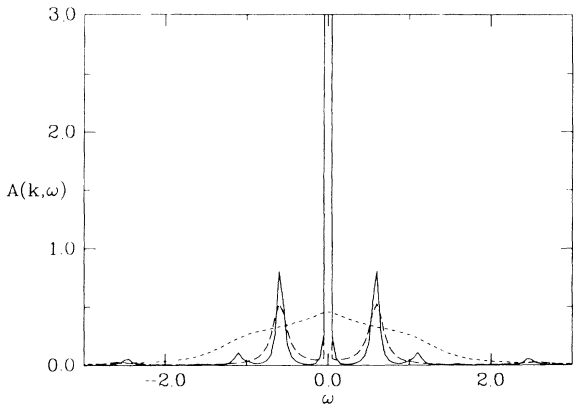

FIG. 9. Plot of the electron spectral function, $A(\mathbf{k},\omega)$ at $(\mathbf{k}=\pi/2,\pi/2)$ vs frequency. The solid and long-dashed curves are obtained from the unrenormalized ME theory from Eq. (23) and Padé approximants, respectively. This gives an idea of the accuracy of the Padé approximants. Note that a quasiparticle peak still exists with spectral weight depleted from the quasiparticle part. The short-dashed curve is obtained via Padé approximants from the renormalized ME theory. In this approximation the spectrum has become entirely incoherent. We used $\lambda_0=1.5$, $\omega_E=0.5$, for a 4×4 system.

versus frequency for $\mathbf{k}=(\pi/2,\pi/2)$, which is on the unperturbed Fermi surface. We have used the usual parameters, $\lambda_0=1.5$ and $\omega_E=0.5$, for a 4×4 system. The solid and long-dashed curves are for the unrenormalized ME theory. The former comes from Eq. (23) with a small artificial smearing, and can be considered exact. The latter follows from Padé approximants. These are presented to give an idea of the accuracy of the Padé approximants. The agreement is excellent considering the sharp structure in the spectral function. The short-dashed curve represents the spectral function obtained by Padé approximants from the renormalized ME theory for the same parameters. The most striking difference is clearly the absence of a quasiparticle peak in the latter case. The entire spectrum is incoherent. In this sense the definition of a mass enhancement via Eq. (16) no longer makes sense since there are no longer quasiparticles. We note from Fig. 9 that a gap at the Fermi level has not yet formed, though the tendency is clearly present, in connection with the results of Fig. 8.

V. CONCLUSIONS

We have studied the Holstein model in two dimensions in a very restricted parameter range in order to evaluate the accuracy of the Migdal-Eliashberg approximation at elevated temperatures. We have used a tight-binding model which gives rise to Fermi surface nesting in two dimensions at half-filling, and we have used an Einstein phonon frequency of order the Fermi energy. All of these conditions are expected to give rise to a breakdown of Migdal's approximation. While it has been clear that there is no superconductivity under the conditions studied here, our results show that there is also no superconductivity predicted with the ME approximation if the

phonon self-energy is self-consistently taken into account. Alternatively, one could use the unrenormalized ME theory but monitor the CDW susceptibility for an instability. However, in order to pursue more quantitative agreement with Monte Carlo results, it was found that the phonon self-energy corrections were necessary and sufficient to take into account. At the elevated temperatures studied in this work, vertex corrections were negligible.

The case presented here ($\lambda_0=1.5$, $\omega_E=0.5$) would appear to be in the weak-coupling regime. However, this is misleading, as the *effective* λ is actually diverging as the CDW instability is approached. Moreover, the electron spectrum becomes entirely incoherent. Since the renormalized ME theory has been successful in the half-filled case, we expect that it can be used with confidence away from half-filling, with possible exceptions arising near the band edges.

ACKNOWLEDGMENTS

The Monte Carlo results were obtained using a program written by J.E. Hirsch. The author is also indebted to him for helpful discussions. The Monte Carlo calculations were performed on the CRAY-XMP at the San Diego Supercomputer Center. This work was supported by the Natural Science and Engineering Research Council (NSERC) of Canada and by the National Science Foundation under Grant No. NSF-DMR-8918306.

APPENDIX

The full set of equations is as follows:

$$\Pi_1(\mathbf{q},i\nu_n)=1+\frac{\nu_n^2}{\omega_E^2}+\frac{2\lambda_0}{N\beta}\sum_{\mathbf{k},m}\frac{[\varepsilon_{\mathbf{k}}+\chi_m(\mathbf{k})][\varepsilon_{\mathbf{k}'}+\chi_{m'}(\mathbf{k}')]-\omega_m\omega_{m'}Z_m(\mathbf{k})Z_{m'}(\mathbf{k}')}{\{\omega_m^2Z_m^2(\mathbf{k})+[\varepsilon_{\mathbf{k}}+\chi_m(\mathbf{k})]^2\}\{\omega_{m'}^2Z_{m'}^2(\mathbf{k}')+[\varepsilon_{\mathbf{k}'}+\chi_{m'}(\mathbf{k}')]^2\}} \tag{A1}$$

and

$$\Pi_2(\mathbf{q},i\nu_n)=\frac{2\lambda_0}{N\beta}\sum_{\mathbf{k},m}\frac{\omega_mZ_m(\mathbf{k})[\varepsilon_{\mathbf{k}'}+\chi_{m'}(\mathbf{k}')]+\omega_{m'}Z_{m'}(\mathbf{k}')[\varepsilon_{\mathbf{k}}+\chi_m(\mathbf{k})]}{\{\omega_m^2Z_m^2(\mathbf{k})+[\varepsilon_{\mathbf{k}}+\chi_m(\mathbf{k})]^2\}\{\omega_{m'}^2Z_{m'}^2(\mathbf{k}')+[\varepsilon_{\mathbf{k}'}+\chi_{m'}(\mathbf{k}')]^2\}}\ , \tag{A2}$$

where $\lambda_0\equiv(\alpha^2/M\omega_E^2)$ and $\mathbf{k}'=\mathbf{k}+\mathbf{q}$, and $\omega_{m'}\equiv\omega_m+\nu_n$, and we have used the shorthand, $Q_m(\mathbf{k})\equiv Q(\mathbf{k},i\omega_m)$. Given that

$$\Pi(\mathbf{q},i\nu_n)=M\omega_E^2\left[\Pi_1(\mathbf{q},i\nu_n)-1-\frac{\nu_n^2}{\omega_E^2}+i\Pi_2(\mathbf{q},i\nu_n)\right]\ , \tag{A3}$$

then the renormalized phonon propagator is determined in terms of the fully interacting electron Green's function by Eqs. (A1) and (A2). This latter quantity is given by

$$\omega_mZ_m(\mathbf{k})=\omega_m+\frac{\lambda_0}{N\beta}\sum_{\mathbf{k}',m'}\frac{\omega_{m'}Z_{m'}(\mathbf{k}')\Pi_1(\mathbf{q},i\nu_n)-[\varepsilon_{\mathbf{k}'}+\chi_{m'}(\mathbf{k}')]\Pi_2(\mathbf{q},i\nu_n)}{[\Pi_1^2(\mathbf{q},i\nu_n)+\Pi_2^2(\mathbf{q},i\nu_n)]\{\omega_{m'}^2Z_{m'}^2(\mathbf{k}')+[\varepsilon_{\mathbf{k}'}+\chi_{m'}(\mathbf{k}')]^2\}} \tag{A4}$$

and

$$\chi_m(\mathbf{k})=-\frac{\lambda_0}{N\beta}\sum_{\mathbf{k}',m'}\frac{\Pi_1(\mathbf{q},i\nu_n)[\varepsilon_{\mathbf{k}'}+\chi_{m'}(\mathbf{k}')]+\Pi_2(\mathbf{q},i\nu_n)\omega_{m'}Z_{m'}(\mathbf{k}')}{[\Pi_1^2(\mathbf{q},i\nu_n)+\Pi_2^2(\mathbf{q},i\nu_n)]\{\omega_{m'}^2Z_{m'}^2(\mathbf{k}')+[\varepsilon_{\mathbf{k}'}+\chi_{m'}(\mathbf{k}')]^2\}}\ , \tag{A5}$$

where $\mathbf{q}\equiv\mathbf{k}-\mathbf{k}'$ and $\nu_n\equiv\omega_m-\omega_{m'}$, and Eq. (6) and the ensuing definition of $\Sigma(\mathbf{k},i\omega_m)$ applies. It turns out that $\Pi_2(\mathbf{q},i\nu_n)$ is zero, so that Eqs. (A4) and (A5) appear as momentum-dependent generalizations of Eqs. (13a) and (13b) in the text, with

$$\lambda_0^{\mathrm{Re}}(\mathbf{q},i\nu_n)\equiv\frac{\lambda_0}{\Pi_1(\mathbf{q},i\nu_n)}\ , \tag{A6}$$

where $\lambda_0^{\mathrm{Re}}(\mathbf{q},i\nu_n)$ is now a phonon propagator (with electron-phonon coupling α^2 included) which has been renormalized by electron-phonon interactions. Equation (A6) can be rewritten

$$\lambda_0^{\mathrm{Re}}(\mathbf{q},i\nu_n)\equiv\frac{\lambda_0(i\nu_n)}{1-\lambda_0(i\nu_n)\chi_0^{\mathrm{CDW}}(\mathbf{q},i\nu_n)}\ , \tag{A7}$$

where

$$\chi_0^{\mathrm{CDW}}(\mathbf{q},i\nu_n)=-\frac{\pi(\mathbf{q},i\nu_n)}{\alpha^2}\ .$$

Equation (A7) clearly illustrates that the CDW tendency is being incorporated into the normal-state self-energy equation.

Momentum dependence in the starting electron-phonon coupling constant is easily incorporated and would alter Eq. (A7) by requiring $\lambda_0(i\nu_n)\rightarrow\lambda_0(\mathbf{q},i\nu_n)$. Equation (A7) is now in a standard RPA form, and one

could define[15] an interaction kernel by Eq. (A7) with coupling constant

$$\lambda_0^{\mathrm{Re}}(\mathbf{q}) \equiv \frac{\lambda_0}{1-\lambda_0 \chi_0^{\mathrm{CDW}}(\mathbf{q},0)} \tag{A8}$$

so that $\lambda_0^{\mathrm{Re}} \equiv \langle \lambda_0^{\mathrm{Re}}(\mathbf{k}-\mathbf{k}') \rangle_{\mathbf{k}\mathbf{k}'}$, where the brackets denote Brillouin-zone averages. We see no reason why this definition should agree quantitatively with the definition (13), although both are expected to behave qualitatively in the same way.

Equation (A7) contains the particle-hole bubble diagrams with *fully* interacting Green's functions. Hence Eqs. (A1), (A2), (A4), and (A5) are iterated to consistency (in one Matsubara frequency and two momentum dimensions). Because, in the process of this iteration, $\Pi_1(\mathbf{q}, i\nu_n)$ approaches zero (see Fig. 6), it is necessary to include a "damping" scheme in the iteration process whereby a combination of the "new" and "old" solution is taken as the new solution, for each iteration step.

[1] J. E. Hirsch and E. Fradkin, Phys. Rev. Lett. **49**, 402 (1982); Phys. Rev. B **27**, 4302 (1983).

[2] R. T. Scalettar, N. E. Bickers, and D. J. Scalapino, Phys. Rev. B **40**, 197 (1989).

[3] A. B. Migdal, Zh. Eksp. Teor. Fiz. **34**, 1438 (1958) [Sov. Phys.—JETP **7**, 996 (1958)]; G. M. Eliashberg, *ibid.* **38**, 966 (1960) [**11**, 696 (1960)].

[4] F. Marsiglio and J. E. Hirsch, Bull. Am. Phys. Soc. **34**, 474 (1989); F. Marsiglio, Physica C **162-164**, 1453 (1989).

[5] P. B. Allen and B. Mitrovic, in *Solid State Physics,* edited by H. Ehrenreich, F. Seitz, and D. Turnbull (Academic, New York, 1982), Vol. 37, p. 1.

[6] J. E. Hirsch and D. J. Scalapino, Phys. Rev. B **32**, 117 (1985).

[7] J. E. Hirsch and D. J. Scalapino, Phys. Rev. Lett. **56**, 2732 (1986).

[8] C. S. Owen and D. J. Scalapino, Physica **55**, 691 (1971).

[9] R. Blankenbecler, D. J. Scalapino, and R. L. Sugar, Phys. Rev. B **24**, 2278 (1981).

[10] J. E. Hirsch, Phys. Rev. B **38**, 12 023 (1988).

[11] F. Marsiglio, M. Schossmann, and J. P. Carbotte, Phys. Rev. B **37**, 4965 (1988).

[12] A. S. Aleksandrov, V. N. Grebenev, and E. A. Mazur, Pis'ma Zh. Eksp. Teor. Fiz. **45**, 357 (1987) [JETP Lett. **45**, 455 (1987)].

[13] A. Moreo, D. J. Scalapino, R. L. Sugar, S. R. White, and N. E. Bickers, Phys. Rev. B **41**, 2313 (1990).

[14] H. J. Vidberg and J. W. Serene, J. Low Temp. Phys. **29**, 179 (1977).

[15] N. E. Bickers, D. J. Scalapino, and R. T. Scalettar, Int. J. Mod. Phys. B **1**, 687 (1987).